Society For Biomaterials

In vivo response to electrochemically aligned collagen bioscaffolds

Vipuil Kishore,[1] Jorge Alfredo Uquillas,[1] Alexandra Dubikovsky,[1] Musa A. Alshehabat,[2] Paul W. Snyder,[2] Gert J. Breur,[2] Ozan Akkus[1]

[1]Weldon School of Biomedical Engineering, Purdue University, West Lafayette, Indiana 47907-2032
[2]School of Veterinary Medicine, Purdue University, West Lafayette, Indiana 47907-2032

Received 21 February 2011; revised 18 July 2011; accepted 5 September 2011
Published online 16 December 2011 in Wiley Online Library (wileyonlinelibrary.com). DOI: 10.1002/jbm.b.31962

Abstract: Collagen-based biomaterials are a viable option for tendon reconstruction and repair. However, the weak mechanical strength of collagen constructs is a major limitation. We have previously reported a novel methodology to form highly oriented electrochemically aligned collagen (ELAC) threads with mechanical properties converging on those of the natural tendon. In this study, we assessed the *in vivo* response of rabbit patellar tendon (PT) to braided ELAC bioscaffolds. Rabbit PTs were incised longitudinally and the ELAC bioscaffold was inlaid in one limb along the length of the tendon. The contralateral limb served as the sham-operated control. Rabbits were euthanized at 4 or 8 months postoperatively. High-resolution radiographs revealed the absence of ectopic bone formation around the bioscaffolds. Four months post-implantation, the histological sections showed that the ELAC bioscaffold underwent limited degradation and was associated with a low-grade granulomatous inflammation. Additionally, quantitative histology revealed that the cross-sectional areas of PTs with the ELAC bioscaffold were 29% larger compared with the controls. Furthermore, ELAC-treated PTs were significantly stiffer compared with the controls. The volume fraction of the tendon fascicle increased in the ELAC-treated PT compared with the controls. By 8 months, the ELAC bioscaffold was mostly absorbed and the enlargement in the area of tendons with implants subsided along with the resolution of the granulomatous inflammation. We conclude that ELAC is biocompatible and biodegradable and has the potential to be used as a biomaterial for tendon tissue engineering applications. © 2011 Wiley Periodicals, Inc. J Biomed Mater Res Part B: Appl Biomater 100B: 400–408, 2012.

Key Words: tendon, tissue engineering, collagen, *in vivo*, granulomatous inflammation

How to cite this article: Kishore V, Uquillas JA, Dubikovsky A, Alshehabat MA, Snyder PW, Breur GJ, Akkus O. 2012. *In vivo* response to electrochemically aligned collagen bioscaffolds. J Biomed Mater Res Part B 2012:100B:400–408.

INTRODUCTION

Tendon injuries pose a significant economical burden to the US each year.[1] Suturing provides satisfactory fixation of soft tissue in tendon and ligament reconstruction. However, these techniques are often associated with difficulties in placement, tissue reconstruction, cutting or pulling through tissue and pull out from bone.[2] Autografts and allografts provide potential alternative strategies, but each of them is associated with limitations such as donor site morbidity[3] and risk of disease transmission from the donor to the recipient, respectively. Therefore, Functional Tissue Engineering strategies have gained considerable interest among researchers as a practical option to treat damaged tendons.[4]

Tissue engineering utilizes a combination of scaffolds and cells to generate functional replacements for damaged tissue. Selection of the biomaterial to be used to fabricate scaffolds critically depends on the specific tissue of interest. Various biomaterials, both natural and synthetic, have been used to fabricate implantable bioscaffolds with the goal of repairing damaged tendons and ligaments.[5–13] Collagen type I, a major component of the tendon extracellular matrix (ECM), is the most widely studied biomaterial for tendon tissue engineering applications.[14–23] Collagen type I forms 70% of tendon's dry weight.[24,25] Law et al. were one of the first groups to evaluate the *in vivo* response of a biomaterial made entirely with type I collagen fibers.[22] They crosslinked the collagen fibers either with glutaraldehyde or by dehydration followed by exposure to cyanamide and reported that the collagen implant showed excellent biocompatibility. Goldstein et al. demonstrated that collagenous tendon prosthesis promoted rapid formation of neo-tendon.[18] Implantation of collagen bioscaffolds seeded with mesenchymal stem cells (MSCs) into the rabbit patellar tendon (PT) has been shown to significantly improve the biomechanical properties of the repair tissue.[15] However, a major concern related to the application of MSCs to promote tendon healing is their

Correspondence to: O. Akkus; e-mail: ozan.akkus@case.edu
Contract grant sponsor: Alfred Mann Institute, Purdue University
Contract grant sponsor: National Institute of Health; contract grant number: NIH 1R21AR056060
Contract grant sponsor: National Science Foundation; contract grant number: CBET-0754442

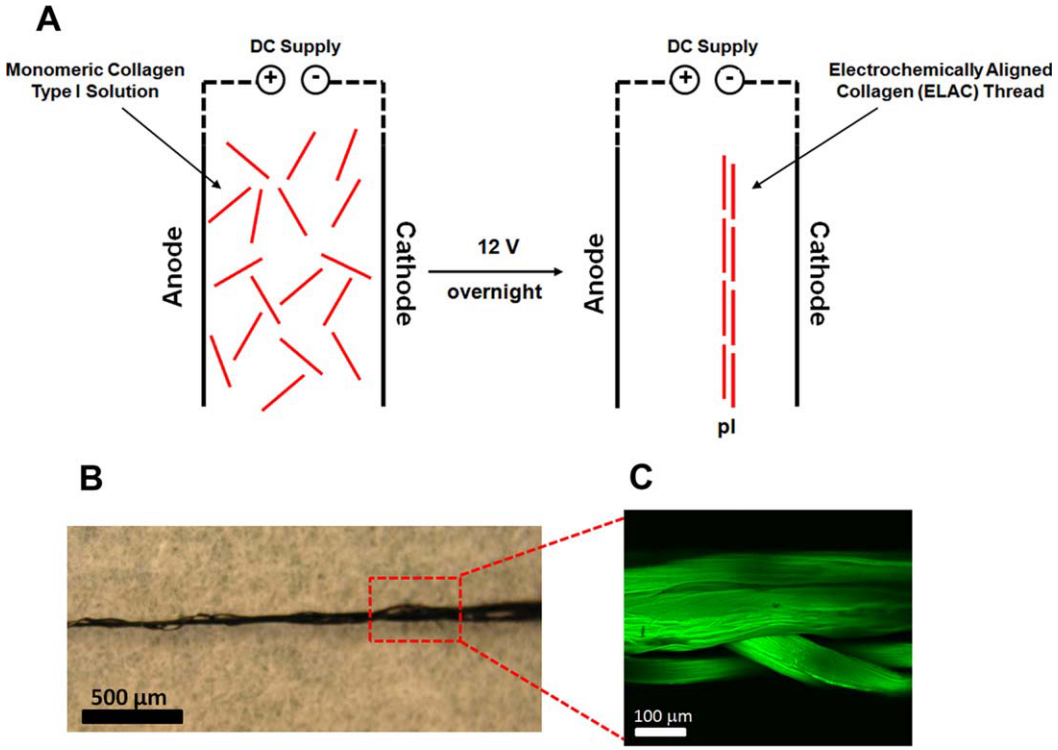

FIGURE 1. A: Schematic explanation of ELAC synthesis. Dialyzed monomeric collagen solution is loaded between two electrodes. On application of 12 V DC, a pH gradient develops between the anode and the cathode. The collagen molecules align along the isoelectric point (pI) to form highly oriented electrochemically aligned collagen (ELAC) threads. B: Photograph of an ELAC triplet formed by braiding three individual ELAC threads together. Three such ELAC triplets were further braided to form the ELAC bioscaffold consisting of nine individual ELAC threads. C) High magnification confocal image of an ELAC triplet. [Color figure can be viewed in the online issue, which is available at wileyonlinelibrary.com.]

tendency to induce ectopic bone formation[14] possibly due to high cell–cell contact and extensive contraction of the collagen gels.[26] Careful selection of cell–collagen ratios have been recommended to prevent the formation of ectopic bone and accelerate tendon healing.[27]

A key limitation of the existing collagen constructs for tendon tissue engineering applications is their weak mechanical strength. For a scaffold to be functional *in vivo*, it needs to be mechanically strong with sufficient compliance to bear daily *in vivo* loads. We have previously developed and reported a novel methodology to align collagen molecules using the principles of isoelectric focusing and form highly oriented and densely packed electrochemically aligned collagen (ELAC) threads.[28] Crosslinking the ELAC thread with genipin resulted in a mechanically strong biomaterial with properties converging upon the native tendon. Genipin is a naturally occurring crosslinking agent (extracted from gardenia fruit), which has been reported to be biocompatible and 10,000 times less cytotoxic compared with glutaraldehyde.[29] Although the *in vitro* degradation and cellular response of ELAC have been investigated,[30] the *in vivo* response of this novel material is unknown. Additionally, little is known about the long-term *in vivo* response to such densely packed collagen-based bioscaffolds. In the current study, we hypothesize that the densely packed ELAC bioscaffold is biocompatible and biodegradable. To test this hypothesis, ELAC bioscaffolds were implanted into the PT of rabbits and the long term *in vivo* response to the material was investigated. Cross-sectional area of tendon, degradation of the scaffold, inflammatory response to the scaffold, and matrix organization of the harvested tissue were examined by qualitative histology, quantitative histology, and immunohistochemistry at 4 or 8 months post-implantation.

MATERIALS AND METHODS

Synthesis of ELAC threads and ELAC bioscaffolds

The ELAC threads were synthesized as previously described.[28] Briefly, acid soluble monomeric collagen solution from bovine hide (Nutragen 6.4 mg/mL; Advanced Biomatrix, Tucson, AZ) was dialyzed with distilled water for 3 days. The dialyzed collagen solution was loaded between two stainless steel wires (electrodes) and an electric voltage of 12 V was applied. In the presence of an electric field, the collagen monomers align along the isoelectric point and form a highly oriented densely packed collagen thread (Figure 1). This ELAC thread was incubated with 10X PBS overnight at 37°C. The ELAC thread was recovered from the electrochemical cells and crosslinked with 0.625% genipin (in 70% ethanol) solution for 3 days at 37°C. Each ELAC thread was about 4 cm in length, 400–500 µm in width and 200–300 µm in thickness.

Three individual genipin crosslinked ELAC threads were manually braided to form an ELAC triplet. Both ends of the ELAC triplet were glued using medical grade adhesive (Loctite 4851). Three individual ELAC triplets were braided again in a similar manner to form the ELAC bioscaffold consisting of nine ELAC threads. As the ELAC bioscaffold is made out of pure collagen, standard medical device sterilization techniques that include physical treatments (UV, gamma radiation, etc.), chemical treatments (ethylene oxide, etc.) and heat treatment (autoclave) were not employed to completely ensure that the collagen structure is not crosslinked or denatured unduly. Given that the genipin crosslinking of the ELAC threads within the scaffold was carried out by using 70% ethanol as the solvent, sterilization of the bioscaffold post-crosslinking was also conducted in the same solvent. After sterilization, the ELAC bioscaffold was washed extensively with DI water to completely remove traces of ethanol and incubated in culture medium (DMEM + 1% penicillin/streptomycin) overnight before surgically implanting it into the PT defects in a rabbit model. At least in this model, the 70% ethanol treatment step for sterilization was efficacious enough that we have not observed infection in any of the rabbits included in the study.

Surgical implantation and PT collection

ELAC bioscaffolds were surgically implanted into the PT of female adult New Zealand white rabbits following an approved protocol by Purdue Animal Care and Use Committee (PACUC). Rabbits were in the range of 2–3 years of age and weighed 4.5 ± 1.0 kg. Rabbits were induced with ketamine, xylazine, and butorphenol (35, 5, and 0.1 mg/kg IM, respectively), intubated, and maintained on a mixture of isoflurane and oxygen. The PT was exposed and a longitudinal incision through the thickness of the tendon was made over the central axis from the patellar to the tibial enthesis, without penetrating the parapatellar fat pad. A 1 mm wide bone trough was burred on the patellar and tibial ends of the PT to facilitate anchoring of the ELAC bioscaffold. On one randomly assigned knee, the ELAC bioscaffold was sandwiched between the medial and lateral strut of the PT and anchored in the troughs using an absorbable tissue adhesive (TissueMed II, Veterinary Products Laboratory, Phoenix, AZ). The longitudinal incision was closed with three or four superficially placed simple interrupted sutures (4-0 PDS, Ethicon). The contralateral knee served as the sham-operated control in which a 1 mm wide bone trough was burred and a longitudinal PT incision was made but the ELAC bioscaffold was not implanted. The animals were euthanized with pentobarbital (1.5 mL IV, Beuthanasia, Schering-Plough Animal Health Corporation) at 4 ($n = 3$) or 8 ($n = 3$) months. Following necropsy, the patella-PT-tibia units were collected for analysis. Each collected unit was evaluated for ectopic bone formation by radiography (Faxitron MX20, 35 kV, 0.3 mA, 300 s). The PT complex was then transected midway between the patella and tibia; the proximal half was used for mechanical testing, and the distal half was fixed in 10% neutral buffered formalin for histology and immunohistochemistry.

Qualitative and quantitative histology

The PT samples for histological evaluation were fixed in 10% neutral buffered formalin. After fixation, the tendon was dehydrated, embedded in paraffin, and cut at 5 μm thickness in transverse direction. Tissue sections were analyzed by qualitative and quantitative histology by staining with hematoxylin and eosin or Masson's trichrome. The cross-sectional area of the entire tendon, the area of the granulomatous inflammatory core (without the ELAC bioscaffold), and the area of the ELAC bioscaffold itself in the experimental knee was measured using perimeter tracing on the sections stained with Masson's trichrome stain. The V_v(fascicle), the volume fraction of the tendon occupied by tendon fascicles, was determined using point counting techniques by overlaying a transparent sheet consisting of an array of points over a Masson trichrome-stained section. The remaining fraction was considered interstitium. All elements of the quantitative analysis were done using an Optiphot-2 microscope (Nikon, Tokyo, Japan) fitted with a computer controlled stage and camera (Optronics, Goleta, CA). Measurements were made using semiautomated image analysis software (Stereo Investigator, MBF Bioscience, Williston, VT).

Immunohistochemistry

Immunohistochemical staining was performed for Type I and Type III collagen. The protocol followed was modified from previously published literature.[31,32] Briefly, the histological sections were deparaffinized with xylene, rehydrated with a graded series of ethanol, and subjected to the following enzymatic treatment for epitope recovery. At first, the sections were incubated with 0.25% trypsin in tris-buffered saline (TBS) with pH = 7.6 at 37°C for 30 min. The tissue sections were then washed with TBS and incubated with hyaluronidase type I-S (1.45 IU/mL) and chondroitinase ABC (0.25 IU/mL) at 37°C for 1 h. After epitope recovery, the sections were washed with TBS and treated with 3% hydrogen peroxide to block endogenous peroxidase activity. Following this, the sections were washed with TBS and incubated with 5% goat serum (in TBS) for 30 min at room temperature to prevent nonspecific binding of the primary antibodies. Rabbit specific primary antibodies for Type I (I-8H5, EMD Chemicals) and Type III (III-53, EMD Chemicals) collagen were diluted in an antibody diluent (Dako, Carpinteria, CA) at a concentration of 10 μg/mL and 100 ng/mL, respectively. The goat serum was drained and the sections were incubated overnight with the primary antibody at room temperature, washed with TBS, and then incubated with a biotinylated anti-mouse secondary antibody (Jackson ImmunoResearch, West Grove, PA) at a dilution of 1:500 (in TBS) for 1 h. After washing with TBS, the sections were incubated with streptavidin-HRP (Jackson ImmunoResearch, West Grove, PA) at a concentration of 2 μg/mL for 30 min. Finally, the sections were completely covered with 3,3′-diaminobenzidine chromogen solution (Dako, Carpinteria, CA) protected from light for 4 min. The sections were then washed with DI water, counterstained with hematoxylin,

and coverslipped. Sections treated similarly but without the primary antibody served as the negative control.

Biomechanical evaluation of matrix modulus

Blocks of harvested tissue samples from the proximal half of the PT were cut transversely to the longer axis of PT (hereafter called as the transverse plane) for biomechanical testing. Samples were wrapped in wet gauze, inserted into a nylon bag, and stored at -20°C until analysis. Each transverse block was about 2-mm-thick. In order to standardize the sample size between the ELAC treated and control PTs, each 2-mm-thick sample was sectioned in the transverse direction with a surgical blade to obtain 1-mm-thick slices. Disc samples were punched out from these slices using 3.5 mm diameter biopsy punches (Miltex, York, PA) using a methodology adopted from Williams et al.[33] In this fashion, two to three cylindrical discs were obtained per transverse slice, resulting in a sample size of $N = 10$–12 in the ELAC-treated group, and $N = 7$–8 in the control group. Immediately after, digital images of the cylindrical discs were obtained to calculate their cross-sectional areas. The cross-sectional area was obtained by processing of digital images of discs by ImageJ Software (Rasband, W.S., ImageJ, US National Institutes of Health, Bethesda, MD). The compression device was custom-built using three translation stages assembled to form an XYZ positioner (CR4500 Series, Parker Automation, Rohnert Park, CA), and a miniature 5-lb load cell (Omega, Stamford, CN). A loading head was mounted to the translation stage. The portion of the loading head contacting the disc sample was a 6 mm hemispherical glass which could freely rotate in 3D (Edmund Optics, Barrington, NJ). The tendon discs were placed in a polycarbonate reservoir containing 1x PBS and the reservoir was mounted on the load cell. Load readings over time were obtained using Lab VIEW (National Instruments, Austin, TX). Each sample was compressed to a displacement corresponding to 50% of its thickness. The thickness was measured by the difference of the displacement at which the loading head contacted the reservoir surface and the displacement at which the loading head engaged the sample (as determined by a reading of 0.1*N*). All samples were compressed at a strain rate of 30% per second. Data were processed in MATLAB (MathWorks, Natick, MA) to calculate the modulus as the slope of the steepest increase of load during initial compression.

Statistical analysis

The cross-sectional areas and the V_v fascicle data of the ELAC treated and the control PTs ($n = 3$/group) at 4 and 8 months were analyzed statistically by using a paired *t*-test. The change in the area of the ELAC bioscaffold and the area of the granulomatous inflammatory core between 4 and 8 months were assessed using a one-tailed two-sample *t*-test. A sample size of $n = 3$ at the observed difference in mean of 0.13 and standard deviation of 0.03 provided a power of 99% for the change in area of the ELAC bioscaffold between 4 and 8 months. Similarly, a sample size of $n = 3$ at the observed difference in mean of 0.40 and standard deviation of 0.18 provided a power of 72% for the change in the area of the granulomatous inflammatory core between 4 and 8 months. The compressive Young's modulus data was analyzed between different treatments (ELAC and Control) and time points (4 and 8 months) using the General Linear Model. If statistical differences were established, a nonparametric Mann-Whitney *U*-test was performed between groups that showed significant differences. Statistical significance threshold was set at $p \leq 0.05$.

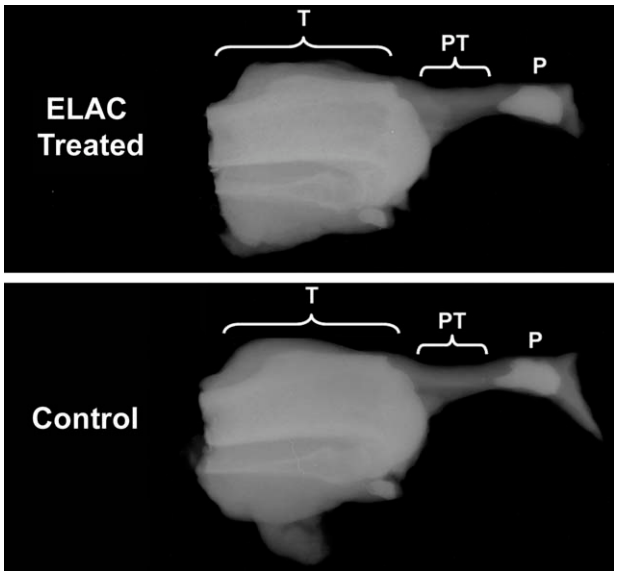

FIGURE 2. Typical radiographic images of ELAC treated and sham-operated control PTs. Ectopic bone calcification was not evident in the tendon proper in both groups at 4 or 8 months post-implantation (P – Patella, T – Tibia, PT – Patellar Tendon).

RESULTS

No ectopic bone formation was observed in the tendon proper in both the ELAC treated PT and the sham-operated control (Figure 2).

Quantitative measurements performed on the Masson trichrome stained sections showed that the cross-sectional areas of the PTs treated with ELAC were about 29% larger ($p = 0.05$) compared to the controls 4 months post-implantation [Figure 3(A)]. The inflammatory core and the implant together accounted for less than 5% of the total tendon area [Figure 3(B)]. By 8 months, the cross-sectional areas of the PTs between the ELAC treated and the control groups were comparable [Figure 3(A)].

At 4 months postoperatively, V_v(fascicle), the percentage of the tendon cross section occupied by tendon fascicles, was higher ($p = 0.10$) in the ELAC group compared the control group (Figure 4).

The ELAC bioscaffold underwent limited degradation between zero and 4 months [Figure 5(A)]. However, between 4 and 8 months, the area of the ELAC bioscaffold decreased significantly ($p = 0.016$) from 0.2 mm^2 at 4 months to less than 0.1 mm^2 by 8 months [Figure 5(A,C,D)]. The granulomatous inflammation area was also observed to

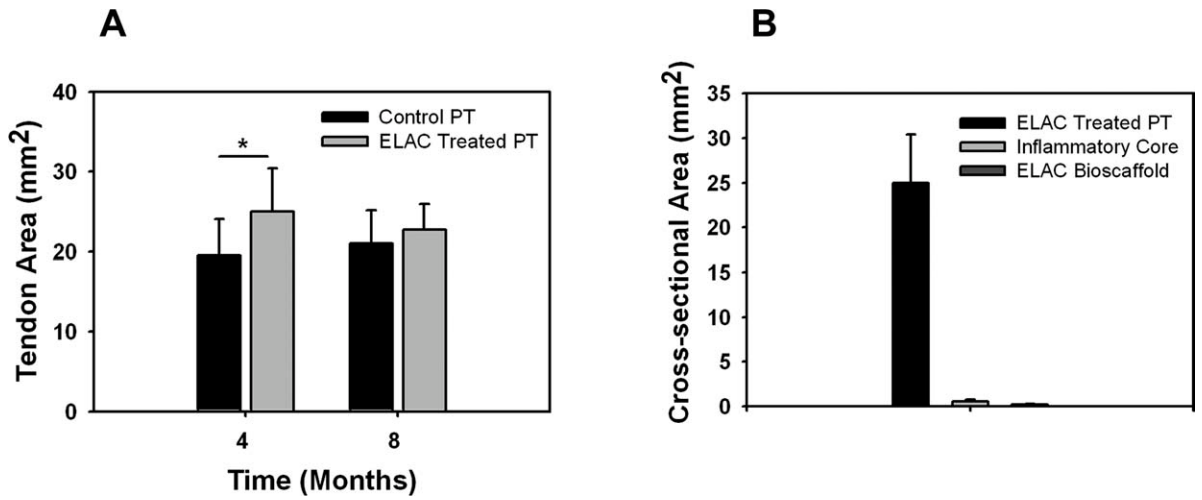

FIGURE 3. Quantification and comparison of the tendon cross-sectional areas between the ELAC treated and sham-operated control PTs. A: The cross-sectional area of the ELAC treated PT was up to 29% greater than the sham-operated control 4 months post-implantation. The lines connecting individual groups indicate statistical significance ($p \leq 0.05$). B: The ELAC bioscaffold and the granulomatous inflammatory core together account for less than 5% of the entire tendon area at the 4-month time point.

significantly decrease ($p = 0.05$) with time from 0.5 mm^2 at 4 months to around 0.1 mm^2 at 8 months (Figure 5(B–D).

Histologically, the inflammation around the ELAC was a low-grade one, comparable with that encountered around the sutures [Figure 5(C)]. This inflammatory core was predominantly populated by macrophages with very few lymphocytes, neutrophils or eosinophils. No foreign body giant cells were found within the inflammatory core. The presence of *de novo* collagenous fibrous connective tissue was evident within the granulomatous inflammatory core 4 months post-implantation [Figure 5(C)]. Immunohistochemistry revealed that this neo tissue formed within the inflammatory core was positive for Type III collagen [Figure 5(E)] and negative for Type I collagen [Figure 5(F)].

The compressive Young's modulus of ELAC treated PTs was significantly greater than ($p = 0.009$) that of control PTs 4 months post-implantation (Figure 6). However, at the 8 months time point the compressive moduli were comparable between the two groups.

DISCUSSION

The current study examined the *in vivo* response of the rabbit PT to a densely packed genipin crosslinked ELAC bioscaffold. The key findings of this study are: (1) The ELAC bioscaffold does not promote ectopic bone calcification at both 4 and 8 months post-implantation. (2) The ELAC bioscaffold degraded with time and was mostly absorbed by 8 months. (3) A low-grade benign granulomatous inflammation predominantly populated by macrophages was evident at 4 months. The area of the granulomatous inflammatory core decreased between 4 and 8 months. (4) The PTs implanted with the ELAC were 29% larger compared to the sham-operated controls 4 months post-implantation. At 8 months, the cross-sectional areas of the PT implanted with the ELAC bioscaffold and the sham-operated control was comparable. (5) The percentage of the tendon cross-section occupied by tendon fascicles, V_v(fascicle), was higher in the ELAC group compared to the control group 4 months postoperatively. No such difference was evident 8 months post transplantation. (6) *De novo* collagenous fibrous tissue positive for Type III collagen was present within the inflammatory niche after 4 months. At 8 months, the granulomatous inflammatory core was mostly resolved. (7) The compressive modulus of ELAC treated PTs at 4 months was stiffer when compared with control tendons. At 8 months, the compressive modulus was comparable between the ELAC treated and sham-operated control PTs.

For anterior cruciate ligament reconstruction, it is standard practice to harvest the central third of the PT and implant these autografts onto the injury site.[34] However, donor site morbidity resulting in suboptimal biomechanical and structural properties is a significant limitation of this approach[35–39] and therefore calls for strategies to restore the harvest site. In an attempt to address this issue, previous studies have employed surgical models in which the

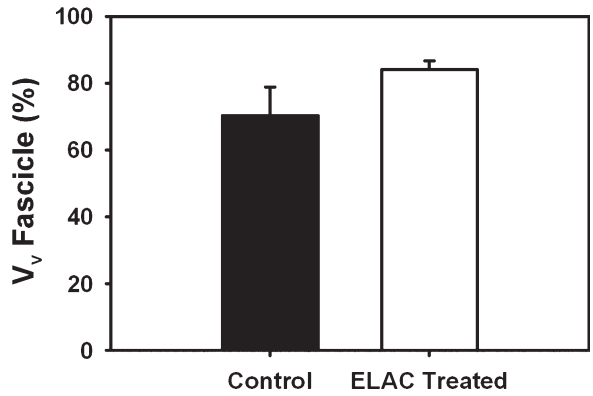

FIGURE 4. Percentage of tendon cross section occupied by fascicles - V_v(fascicle) - 4 months postimplantation. The V_v(fascicle) was higher in the ELAC treated PTs compared to the sham-operated controls.

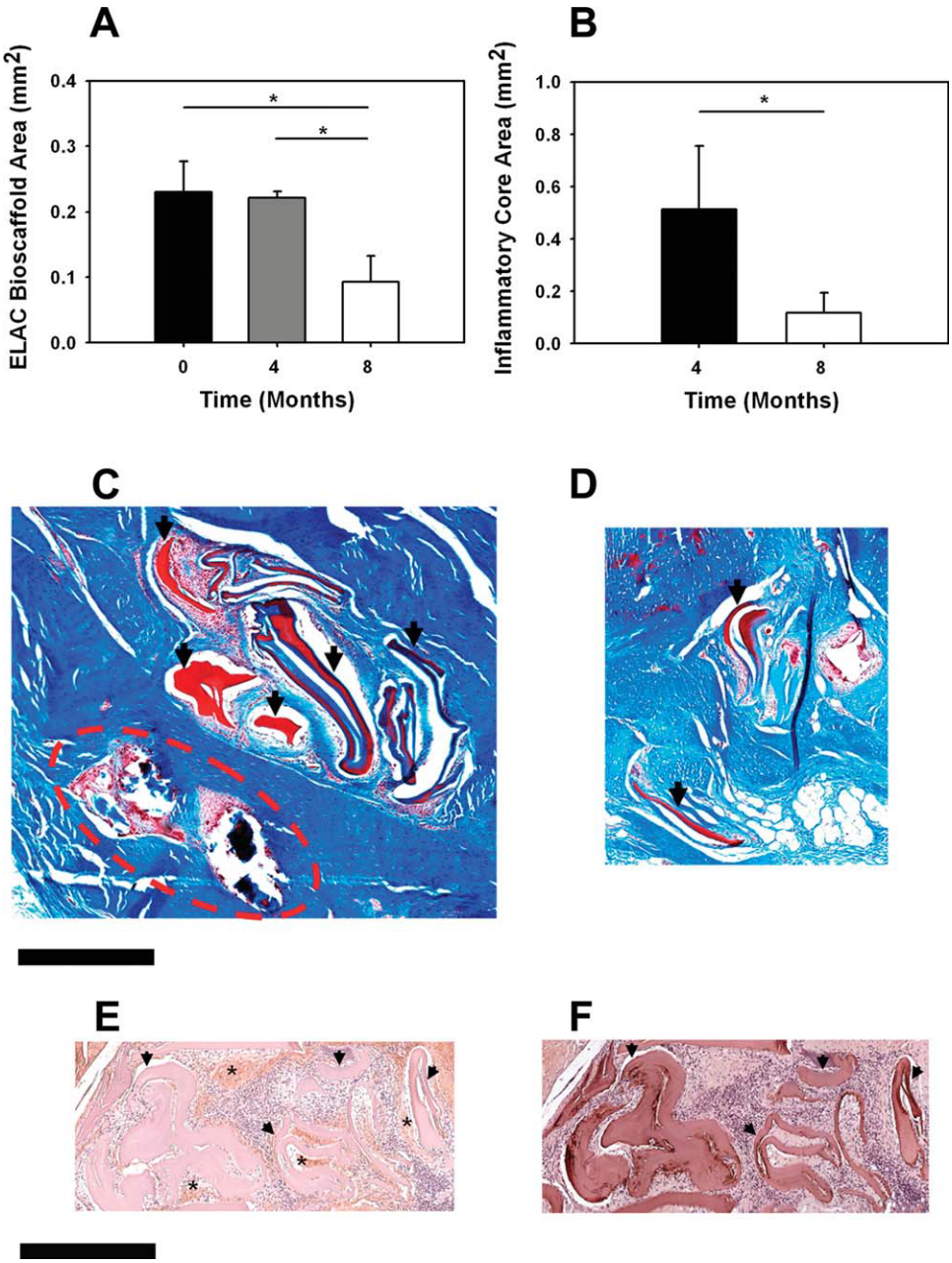

FIGURE 5. Histological and immunohistochemical characterization of the ELAC treated PTs. Quantitative histology indicated that (A) the area of the ELAC bioscaffold decreases significantly after 4 months and is mostly absorbed by the end of 8 months and (B) the area of the granulomatous inflammatory core also reduces significantly with time and is largely resolved by 8 months. The lines connecting individual groups indicate statistical significance ($p \leq 0.05$). C, D: High magnification images of the granulomatous inflammatory core (C) at 4 months and (D) at 8 months post-implantation. The 'arrow heads' point to the ELAC bioscaffold and the dotted ellipse surrounds the sutures. Scale bar: 0.5 mm. E, F: Immunohistochemical images of the ELAC treated PTs 4 months post-implantation stained with (E) Type III collagen and (F) Type I collagen. The *de novo* collagenous fibrous tissue formed within the granulomatous inflammatory niche was positive for Type III collagen and negative for Type I collagen. The 'arrow heads' point to the ELAC bioscaffold and '*' indicates the *de novo* collagenous fibrous tissue formed within the granulomatous inflammatory niche. Scale bar: 0.5 mm. [Color figure can be viewed in the online issue, which is available at wileyonlinelibrary.com.]

central third of the PT is removed and efforts are made to restore the injury site using natural[9] or synthetic materials[14,19] with or without cells. Healing in such surgical models require significant regeneration of the lost tissue to regain full functionality. In contrast, the surgical model employed in the current study is less invasive. Although a longitudinal incision was made along the length of the PT, no part of the tissue was harvested during surgery. Healing involved closure of the wound, body's response to the foreign material and the integration/degradation of the scaffold within the tendon proper. This surgical model was chosen for the current study to solely evaluate the *in vivo* response

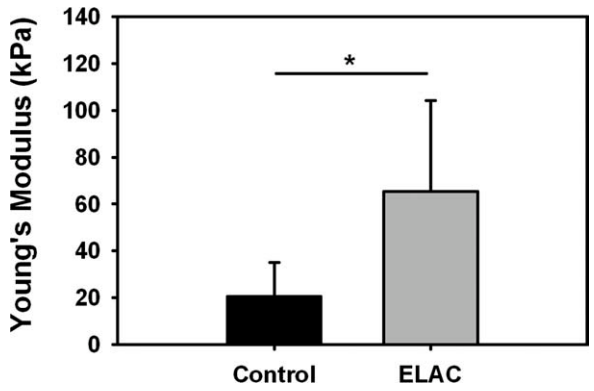

FIGURE 6. Compressive Young's Modulus of the ELAC treated and control PTs 4 months post-implantation. The lines connecting individual groups indicate statistical significance ($p \leq 0.05$). The Young's modulus of the ELAC treated PTs was significantly greater than that of the sham-operated controls.

of the tendon proper to the novel biomaterial. Otherwise, reconstructing the tendon proper was not an immediate aim of the current study.

Autografts and allografts have been used in PT reconstructive surgery.[40,41] Patella-quadriceps tendon has been used as an autograft to reconstruct damaged PT.[41] However, application of autografts for tendon repair is limited due to problems such as donor site morbidity and the need for multiple surgeries.[3] In the context of allografts, successful application of allograft patellar ligament for PT reconstruction has been demonstrated.[40] Nonetheless, concerns still exist about the biological traces of DNA left in the allograft which can be a cause of disease transmission and immunogenic response.[42] Therefore, tissue engineering is a viable strategy for tendon reconstruction and repair.

One of the most critical parameters of tissue engineering is that the rate of degradation of the implant needs to correlate closely with the formation of the *de novo* tissue.[43] Autologous MSC-collagen composites have been reported to significantly improve the biomechanical properties of the repair tissue.[14] However, ectopic bone formation was observed in 28% of MSC-collagen grafted tendons. To circumvent bone formation, excessive construct contraction was reduced by using low cell densities.[19] In the current study, a pure collagen based scaffold devoid of any cells was implanted into a PT defect and no ectopic bone formation was observed at the repair site up to 8 months post-implantation (Figure 2). In the context of macroscopic collagen fiber-based bioscaffolds, Law et al. crosslinked collagen fibers either via dehydrothermal/cyanamide (DHT/C) or by exposing them to glutaraldehyde vapor.[22] They reported that collagen fibers crosslinked by DHT/C degraded rapidly and by 6 weeks very little of the implant was remaining. Since typical healing times for tendon injuries post surgery range from 3–6 months, rapid degradation of collagen fibers via DHT/C crosslinking might not be optimal for tendon repair. On the other hand, glutaraldehyde crosslinked collagen fibers absorbed much slower and remained for up to 6 months post-implantation. The cytotoxic nature of glutaraldehyde crosslinking might make the implant vulnerable to several complications post-implantation.[29] Goldstein et al. investigated *in vivo* response of rabbit Achilles tendon to type I collagen fiber implants crosslinked either with glutaraldehyde or with dehydrothermal treatment followed by carbodiimide.[18] Although the glutaraldehyde crosslinked implants appeared to degrade minimally by 20 weeks, the carbodiimide crosslinked implants were mostly absorbed by 10 weeks. Additionally, the carbodiimide crosslinked implants were reported to promote rapid formation of neotendon. In the current study, remnants of genipin crosslinked ELAC bioscaffold were present 8 months post-implantation. The slow degradation rate of the ELAC implant compared to the carbodiimide crosslinked and cynamide crosslinked implants used in the aforementioned studies might be due to genipin introduced inter-microfibrillar crosslinks between adjacent collagen microfibrils.[44] The rate of degradation of the ELAC bioscaffold can be controlled by optimizing the degree of crosslinking[45] by varying different parameters like the concentration of genipin used, duration of crosslinking, and the solvent used (ethanol vs. PBS).

The cross-sectional areas of the PTs implanted with the ELAC bioscaffold were significantly larger compared with the sham-operated controls 4 months post-implantation [Figure 3(A)]. As the ELAC bioscaffold and the granulomatous inflammatory core contribute to less than 5% of the total tendon area [Figure 3(B)], the increase in tendon area was due to the enlargement of the existing tendon. This increase in tendon area was accompanied with an increase in the volume fraction of fascicles (Figure 4). Given that the implant itself lacked bioinductive factors, a plausible explanation for the observed anabolism of the tendon could be associated with the factors released locally by the granulomatous inflammation. In support of this postulation, the cross-sectional areas of the ELAC treated and the sham-operated controls became comparable as the granulomatous area declined [Figure 3(B)]. It is difficult to determine the mechanism of enlargement of the ELAC treated PTs at 4 months due to the absence of earlier time points. The reduction is tendon area between 4 and 8 months after surgery suggests that the healing process was in its remodeling phase. Further studies which include earlier time points that include the reparative phase of the tendon healing process are needed to conclusively understand the mechanisms involved behind the observed enlargement in the cross-sectional area of the ELAC treated PT. While the results imply that the anabolic effect is linked to the low-grade prolonged granulomatous inflammation, blockage of the granulomatous response will definitively demonstrate whether a cause–effect relation exists between the inflammatory core and the anabolic response in tendon.

Histological analysis of the harvested tissue 4 months post-implantation revealed the presence of a low-grade granulomatous inflammation[46] around the perimeter of the ELAC bioscaffold [Figure 5(C)]. This granulomatous core was mainly comprised of macrophages and fewer lymphocytes, neutrophils and eosinophils but was devoid of foreign body giant cells. This is contrary to a previous study that

reported the presence of foreign body giant cells actively involved in the phagocytosis of the collagen implant from as early as 10 days up to 6 months post-implantation.[22] This might be due to the differences in the size of the implant and the crosslinking agents used between studies. The granulomatous inflammation observed in the present study was similar to that reported for injectable collagen implants used as facial fillers to correct for scarring and wrinkles.[47–50] The scarcity of neutrophils and eosinophils within the inflammatory core suggests that the sterilization procedure adopted prior to the surgical implantation of the ELAC bioscaffold was adequate and that degradation byproducts were not eliciting acute inflammation. The granulomatous inflammatory core was negative for collagen type I and rich in collagen type III at 4 months indicating the replacement of inflammation with scar tissue [Figure 5(E,F)]. This is in agreement with previous studies using MSC-collagen composites that report strong staining of collagen types III and V twelve weeks post-implantation.[19] The decrease in the area of the granulomatous inflammatory core by 8 months was coupled with a reduction in tendon area indicating an ongoing remodeling of the scar tissue.

There are two limitations to the current study. First, as the aim of the current study was to solely evaluate the *in vivo* response to a novel collagen-based bioscaffold within the tendon proper, the changes in the construct attachment site were not investigated. Although the implant was anchored into the bone at both the patella and tibial ends using a tissue adhesive, it was merely done to hold the implant within the tendon proper. Future studies will focus on the development of the ELAC bioscaffold with a goal to efficiently anchor the construct into the bone insertion sites. The efficacy of the construct attachment and the changes in the attachment site will be investigated via biomechanical testing and histological analysis.

The second limitation of the current study is that biomechanical evaluation of the whole PTs with the construct was not performed due to limited sample size. However, compression biomechanical testing on disc shaped slices of tendon was performed to evaluate the effects of the ELAC bioscaffold on the neighboring tendon stiffness (Figure 6). Therefore, albeit not physiologically relevant, the method used here allowed assessing the effects of the implant. Others have also utilized compression to observe compressive stiffness of the bursal and articular sides of the supraspinatus tendon.[51] Williams et al. studied the anisotropic compressive mechanical properties of the rabbit PT in the transverse and longitudinal direction of tendon fibers.[33] They found the compressive modulus at strain rates of 10% per second in the longitudinal direction as 3.26 ($\pm$3.49) kPa. This value is smaller than the longitudinal compressive modulus of our control group at 4 months: 20.46 ($\pm$14.67) kPa. However, it is known that in viscoelastic solids such as tendons the stress increases as the applied strain rate increases. The strain rate used in the current study is about three times higher than that used by Williams et al. which might explain the difference in modulus. Additionally, Williams et al. computed compressive moduli in small strain regions of the monotonic loading curves where as in the current study the compressive moduli of the time-dependent stress curves were calculated in the region of the steepest slope. The increased moduli in the tendon from PTs implanted with ELAC are likely due to changes in the matrix composition as seen in the increased fascicle volume fraction in ELAC-treated PTs at 4 months (Figure 4). Secretion of collagen and various proteoglycans from the resident tendon cells may have resulted in a stiffer matrix which remains to be confirmed by analyzing the expression of ECM molecules by real-time PCR as well as biochemical analysis of the ECM.

In conclusion, this study demonstrates that the ELAC bioscaffold when implanted in a rabbit PT model: (a) degrades over a time scale of months, (b) does not promote ectopic bone formation, (c) does not induce severe inflammatory reaction, and (d) increases the volume fraction of the fascicles within the tendon proper. Therefore, ELAC has the potential to be translated to the clinical environment for the regeneration of atrophied musculoskeletal tissues.

ACKNOWLEDGMENTS

The authors thank Carol Bain at Purdue University Histopathology service laboratory for her help with the histological work.

REFERENCES

1. Praemer A, Furner S, Rice D. Musculoskeletal condition in the United States. Am Acad Orthop Surg 1992.
2. Krackow KA, Thomas SC, Jones LC. Ligament-tendon fixation: Analysis of a new stitch and comparison with standard techniques. Orthopedics 1988;11:909–917.
3. Kartus J, Movin T, Karlsson J. Donor-site morbidity and anterior knee problems after anterior cruciate ligament reconstruction using autografts. Arthroscopy 2001;17:971–980.
4. Butler DL, Juncosa-Melvin N, Boivin GP, Galloway MT, Shearn JT, Gooch C, Awad H. Functional tissue engineering for tendon repair: A multidisciplinary strategy using mesenchymal stem cells, bioscaffolds, and mechanical stimulation. J Orthop Res 2008;26:1–9.
5. Cooper JA, Lu HH, Ko FK, Freeman JW, Laurencin CT. Fiber-based tissue-engineered scaffold for ligament replacement: Design considerations and in vitro evaluation. Biomaterials 2005;26: 1523–1532.
6. Fan H, Liu H, Toh SL, Goh JC. Anterior cruciate ligament regeneration using mesenchymal stem cells and silk scaffold in large animal model. Biomaterials 2009;30:4967–4977.
7. Fan H, Liu H, Wong EJ, Toh SL, Goh JC. In vivo study of anterior cruciate ligament regeneration using mesenchymal stem cells and silk scaffold. Biomaterials 2008;29:3324–3337.
8. Funakoshi T, Majima T, Iwasaki N, Suenaga N, Sawaguchi N, Shimode K, Minami A, Harada K, Nishimura S. Application of tissue engineering techniques for rotator cuff regeneration using a chitosan-based hyaluronan hybrid fiber scaffold. Am J Sports Med 2005;33:1193–1201.
9. Karaoglu S, M BF, Woo SL, Fu YC, Liang R, Abramowitch SD. Use of a bioscaffold to improve healing of a patellar tendon defect after graft harvest for ACL reconstruction: A study in rabbits. J Orthop Res 2008;26:255–263.
10. Lu HH, Cooper JA, Jr, Manuel S, Freeman JW, Attawia MA, Ko FK, Laurencin CT. Anterior cruciate ligament regeneration using braided biodegradable scaffolds: In vitro optimization studies. Biomaterials 2005;26:4805–4816.
11. Moffat KL, Kwei AS, Spalazzi JP, Doty SB, Levine WN, Lu HH. Novel nanofiber-based scaffold for rotator cuff repair and augmentation. Tissue Eng Part A 2009;15:115–126.

12. Ouyang HW, Goh JC, Thambyah A, Teoh SH, Lee EH. Knitted poly-lactide-co-glycolide scaffold loaded with bone marrow stromal cells in repair and regeneration of rabbit Achilles tendon. Tissue Eng 2003;9:431–439.
13. Yokoya S, Mochizuki Y, Nagata Y, Deie M, Ochi M. Tendon-bone insertion repair and regeneration using polyglycolic acid sheet in the rabbit rotator cuff injury model. Am J Sports Med 2008;36:1298–1309.
14. Awad HA, Boivin GP, Dressler MR, Smith FN, Young RG, Butler DL. Repair of patellar tendon injuries using a cell-collagen composite. J Orthop Res 2003;21:420–431.
15. Awad HA, Butler DL, Boivin GP, Smith FN, Malaviya P, Huibregtse B, Caplan AI. Autologous mesenchymal stem cell-mediated repair of tendon. Tissue Eng 1999;5:267–277.
16. Chvapil M, Speer DP, Holubec H, Chvapil TA, King DH. Collagen fibers as a temporary scaffold for replacement of ACL in goats. J Biomed Mater Res 1993;27:313–325.
17. Fini M, Torricelli P, Giavaresi G, Rotini R, Castagna A, Giardino R. In vitro study comparing two collageneous membranes in view of their clinical application for rotator cuff tendon regeneration. J Orthop Res 2007;25:98–107.
18. Goldstein JD, Tria AJ, Zawadsky JP, Kato YP, Christiansen D, Silver FH. Development of a reconstituted collagen tendon prosthesis. A preliminary implantation study. J Bone Joint Surg Am 1989;71:1183–1191.
19. Juncosa-Melvin N, Boivin GP, Gooch C, Galloway MT, West JR, Dunn MG, Butler DL. The effect of autologous mesenchymal stem cells on the biomechanics and histology of gel-collagen sponge constructs used for rabbit patellar tendon repair. Tissue Eng 2006; 12:369–379.
20. Koob TJ, Willis TA, Hernandez DJ. Biocompatibility of NDGA-polymerized collagen fibers. I. Evaluation of cytotoxicity with tendon fibroblasts in vitro. J Biomed Mater Res 2001;56:31–39.
21. Koob TJ, Willis TA, Qiu YS, Hernandez DJ. Biocompatibility of NDGA-polymerized collagen fibers. II. Attachment, proliferation, and migration of tendon fibroblasts in vitro. J Biomed Mater Res 2001;56:40–48.
22. Law JK, Parsons JR, Silver FH, Weiss AB. An evaluation of purified reconstituted type 1 collagen fibers. J Biomed Mater Res 1989;23:961–977.
23. Young RG, Butler DL, Weber W, Caplan AI, Gordon SL, Fink DJ. Use of mesenchymal stem cells in a collagen matrix for Achilles tendon repair. J Orthop Res 1998;16(4):406–13.
24. Amiel D, Frank C, Harwood F, Fronek J, Akeson W. Tendons and ligaments: a morphological and biochemical comparison. J Orthop Res 1984;1(3):257–65.
25. Fujii K, Yamagishi T, Nagafuchi T, Tsuji M, Kuboki Y. Biochemical properties of collagen from ligaments and periarticular tendons of the human knee. Knee Surg Sports Traumatol Arthrosc 1994;2: 229–233.
26. Harris MT, Butler DL, Boivin GP, Florer JB, Schantz EJ, Wenstrup RJ. Mesenchymal stem cells used for rabbit tendon repair can form ectopic bone and express alkaline phosphatase activity in constructs. J Orthop Res 2004;22:998–1003.
27. Juncosa-Melvin N, Boivin GP, Galloway MT, Gooch C, West JR, Sklenka AM, Butler DL. Effects of cell-to-collagen ratio in mesenchymal stem cell-seeded implants on tendon repair biomechanics and histology. Tissue Eng 2005;11(3–4):448–457.
28. Cheng X, Gurkan UA, Dehen CJ, Tate MP, Hillhouse HW, Simpson GJ, Akkus O. An electrochemical fabrication process for the assembly of anisotropically oriented collagen bundles. Biomaterials 2008;29:3278–3288.
29. Sung HW, Huang RN, Huang LL, Tsai CC. In vitro evaluation of cytotoxicity of a naturally occurring cross-linking reagent for biological tissue fixation. J Biomater Sci Polym Ed 1999;10:63–78.
30. Gurkan UA, Cheng X, Kishore V, Uquillas JA, Akkus O. Comparison of morphology, orientation, and migration of tendon derived fibroblasts and bone marrow stromal cells on electrochemically aligned collagen constructs. J Biomed Mater Res A 2010;94: 1070–1079.
31. Kumagai J, Sarkar K, Uhthoff HK. The collagen types in the attachment zone of rotator cuff tendons in the elderly: An immunohistochemical study. J Rheumatol 1994;21:2096–2100.
32. Kumagai J, Sarkar K, Uhthoff HK, Okawara Y, Ooshima A. Immunohistochemical distribution of type I, II and III collagens in the rabbit supraspinatus tendon insertion. J Anat 1994;185 (Pt 2): 279–284.
33. Williams LN, Elder SH, Bouvard JL, Horstemeyer MF. The anisotropic compressive mechanical properties of the rabbit patellar tendon. Biorheology 2008;45:577–586.
34. Tomita F, Yasuda K, Mikami S, Sakai T, Yamazaki S, Tohyama H. Comparisons of intraosseous graft healing between the doubled flexor tendon graft and the bone-patellar tendon-bone graft in anterior cruciate ligament reconstruction. Arthroscopy 2001;17: 461–476.
35. Atkinson TS, Atkinson PJ, Mendenhall HV, Haut RC. Patellar tendon and infrapatellar fat pad healing after harvest of an ACL graft. J Surg Res 1998;79:25–30.
36. Beynnon BD, Proffer D, Drez DJ, Jr, Stankewich CJ, Johnson RJ. Biomechanical assessment of the healing response of the rabbit patellar tendon after removal of its central third. Am J Sports Med 1995;23:452–457.
37. Burks RT, Haut RC, Lancaster RL. Biomechanical and histological observations of the dog patellar tendon after removal of its central one-third. Am J Sports Med 1990;18:146–153.
38. Miyashita H, Ochi M, Ikuta Y. Histological and biomechanical observations of the rabbit patellar tendon after removal of its central one-third. Arch Orthop Trauma Surg 1997;116:454–462.
39. Proctor CS, Jackson DW, Simon TM. Characterization of the repair tissue after removal of the central one-third of the patellar ligament. An experimental study in a goat model. J Bone Joint Surg Am 1997;79:997–1006.
40. Cushing MV, Lundy DW, Keating JG, Ogden JA. Patellar ligament reconstruction using allograft patellar ligament: a case report. Am J Orthop (Belle Mead NJ) 1999;28:263–266.
41. Williams RJ, III, Brooks DD, Wickiewicz TL. Reconstruction of the patellar tendon using a patella-quadriceps tendon autograft. Orthopedics 1997;20:554–558.
42. Eastlund T. Bacterial infection transmitted by human tissue allograft transplantation. Cell Tissue Bank 2006;7:147–166.
43. Liu Y, Ramanath HS, Wang DA. Tendon tissue engineering using scaffold enhancing strategies. Trends Biotechnol 2008;26:201–209.
44. Sung HW, Chang WH, Ma CY, Lee MH. Crosslinking of biological tissues using genipin and/or carbodiimide. J Biomed Mater Res A 2003;64:427–438.
45. Liang HC, Chang Y, Hsu CK, Lee MH, Sung HW. Effects of crosslinking degree of an acellular biological tissue on its tissue regeneration pattern. Biomaterials 2004;25:3541–3552.
46. Williams GT, Williams WJ. Granulomatous inflammation—A review. J Clin Pathol 1983;36:723–733.
47. Alcalay J, Alkalay R, Gat A, Yorav S. Late-onset granulomatous reaction to Artecoll. Dermatol Surg 2003;29:859–862.
48. Barr RJ, Stegman SJ. Delayed skin test reaction to injectable collagen implant (Zyderm). The histopathologic comparative study. J Am Acad Dermatol 1984;10:652–658.
49. Overholt MA, Tschen JA, Font RL. Granulomatous reaction to collagen implant: Light and electron microscopic observations. Cutis 1993;51:95–98.
50. Swanson NA, Stoner JG, Siegle RJ, Solomon AR. Treatment site reactions to Zyderm Collagen Implantation. J Dermatol Surg Oncol 1983;9:377–380.
51. Lee SB, Nakajima T, Luo ZP, Zobitz ME, Chang YW, An KN. The bursal and articular sides of the supraspinatus tendon have a different compressive stiffness. Clin Biomech (Bristol, Avon) 2000; 15:241–247.